INTERNATIONAL JOURNAL FOR NUMERICAL METHODS IN FLUIDS
Int. J. Numer. Meth. Fluids **28**: 1355–1369 (1998)

SIMULATION OF THREE-DIMENSIONAL POLYMER MOULD FILLING PROCESSES USING A PSEUDO-CONCENTRATION METHOD

G.A.A.V. HAAGH AND F.N. VAN DE VOSSE*

Eindhoven University of Technology, Centre of Polymers and Composites, PO Box 513, 5600 MB Eindhoven, Netherlands

SUMMARY

Mould filling processes, in which a material flow front advances through a mould, are typical examples of moving boundary problems. The moving boundary is accompanied by a moving contact line at the mould walls causing, from a macroscopic modelling viewpoint, a stress singularity. In order to be able to simulate such processes, the moving boundary and moving contact line problem must be overcome. A numerical model for both two- and three-dimensional mould filling simulations has been developed. It employs a pseudo-concentration method in order to avoid elaborate three-dimensional remeshing, and has been implemented in a finite element program. The moving contact line problem has been overcome by employing a Robin boundary condition at the mould walls, which can be turned into a Dirichlet (no-slip) or a Neumann (free-slip) boundary condition depending on the local pseudo-concentration. Simulation results for two-dimensional test cases demonstrate the model's ability to deal with flow phenomena such as fountain flow and flow in bifurcations. The method is by no means limited to two-dimensional flows, as is shown by a pilot simulation for a simple three-dimensional mould. The reverse problem of mould filling is the displacement of a viscous fluid in a tube by a less viscous fluid, which has had considerable attention since the 1960's. Simulation results for this problem are in good agreement with results from the literature. © 1998 John Wiley & Sons, Ltd.

KEY WORDS: viscous flow; moving boundary; fountain flow; pseudo-concentration method; finite element method

1. INTRODUCTION

A major aim of the simulation of mould filling processes is to predict the trajectories of fluid particles including the development of the flow front. This flow front is a moving free surface, of which the position is to be determined as part of the solution procedure. The contact lines of the free surface at the mould walls are also moving, giving rise to extra complications, such as a stress singularity at the contact line in case of a no-slip boundary condition for the filling fluid [1].

Several methods have been developed to solve problems of viscous flows with moving boundaries [2–4]. Adaptive grid methods (involving remeshing) have been commonly used in codes for two-dimensional simulation of moulding processes: the mesh covers the fluid area and is extended upon every time step.

* Correspondence to: Centre for Polymers and Composites, Eindhoven University of Technology, PO Box 513, 5600 MB Eindhoven, Netherlands.

CCC 0271–2091/98/191355–15$17.50

Received March 1997
Revised September 1997

Our interest is focused on three-dimensional mould filling simulations, for which we have chosen to avoid remeshing, since it is very elaborate for three-dimensional meshes. Instead, we have adopted a pseudo-concentration method [5], which is related to the volume of fluid (VOF) method [6]. In this method, the flow problem is solved on a fixed grid that covers the entire mould. A fictitious fluid is introduced to represent the air downstream of the flow front. The main property of this fictitious fluid is that it should not contribute to the pressure build-up in the mould during filling. Therefore, its viscosity is set to a value at least 10^3 times smaller than the viscosity of the filling fluid. However, the viscosity of the fictitious fluid exceeds the real value for air by several orders in order to keep the Reynolds number small. Furthermore, the fictitious fluid is allowed to leave the mould at some specified boundaries.

The distinction between filling fluid and fictitious fluid is made by labelling fluid particles with a material label c (being the pseudo-concentration), which is given the value $c = 1$ for the filling fluid, and $c = 0$ for the fictitious fluid. Near the flow front, c is a continuous function between 1 and 0; the flow front itself is determined by the iso-value line for $c = 0.5$. This interface is tracked by convecting the material labels with the fluid velocity.

In viscous flows, the region immediately upstream of the flow front is characterised by the fountain flow phenomenon [7]: fluid particles that approach the front from the (upstream) core of the flow, are diverted towards the wall. In the past, approximate solutions were developed for fountain flow (under the assumption of a flat flow front) in an axisymmetric cylinder [8] and between two parallel plates [9]. However, no such expressions for fountain flow in three-dimensional moulds are available.

The pseudo-concentration method has also been used in the context of mould filling by others, [3–5,10–12] who use different boundary conditions at the mould walls. Thompson [5] imposes a no-slip condition at the mould wall parts that are wetted by the filling fluid, but he is not clear about the boundary condition in the fictitious fluid. His mould filling example shows a moving contact line that is considerably lagging behind with respect to the flow front. His pseudo-concentration function is a continuously decreasing function that has to be smoothed regularly because it is severely distorted by the convection algorithm. Moreover, he reports a mass loss of 10%. Lewis and co-workers [3,10] adopt the method for the two-dimensional simulation of metal casting. However, they approach the turbulent metal flow as a laminar flow with a free-slip boundary condition at the entire mould wall. Hence the fountain flow effect, which is irrelevant to their case, does not occur. Fortin *et al.* [11] also use the pseudo-concentration method for two-dimensional (polymer) injection moulding. Prescribing no-slip for the filling fluid, and free stress in both normal and tangential direction for the fictitious fluid, they are able to capture the fountain flow effect. Their attempts to impose a zero normal velocity for the fictitious fluid along the mould walls (except at specified air vents) failed, as this resulted in a thin layer of fictitious fluid remaining at the wall after the flow front had passed (A. Fortin, personal communication). Hétu *et al.* [12] use the same boundary conditions as Fortin *et al.* Their flow front results seem rather inaccurate—with material appearing at locations in the mould that have not been reached by the flow front yet—and they do not show any fountain flow results. Finally, Medale and Jaeger [4] solve the pseudo-concentration convection equation only in a limited domain surrounding the interface. They then correct for mass losses by slightly changing the value of the material label $c_{\text{interface}}$ that determines the interface position. At the mould walls, the following slip condition is imposed:

$$\tau_{\text{wall}} = -f u_{\text{t}}, \tag{1}$$

in which τ_{wall} is the wall shear stress, u_t is the velocity tangential to the wall, and f is a friction coefficient which is set to 0.01.

In this paper we want to demonstrate that the pseudo-concentration method is suitable to simulate the filling of a mould with a Newtonian fluid when the proper boundary conditions are applied. First, the results for a two-dimensional (axisymmetric) mould will be shown to prove that the method captures the important aspects of the flow, such as the flow front shape and the fountain flow effect. Therefore, our model for mould filling simulations is presented in Section 2. Special attention is given to the boundary conditions, which strongly influence the movement of the contact points (or lines). In this paper, we will not take into account surface tension and non-isothermal effects. The implementation of the model in a finite element code is treated in Section 3. In Section 4 a number of simulation results will be discussed, leading to the conclusions given in Section 5.

As an example of moulding processes, the injection moulding of polymer products will be considered. Consequently, the filling fluid will be referred to as 'polymer'. However, the method employed here is—in principle—also applicable to other moulding processes.

2. MODELLING

In this section the model for three-dimensional mould filling simulations will be derived from the equations governing the process. It will be shown that the boundary and interface conditions require special attention.

2.1. Governing equations

For the sake of simplicity, the flow is considered incompressible and isothermal, hence the conservation equations for mass and momentum reduce to the Navier–Stokes equations:

$$\nabla \cdot \mathbf{u} = 0, \tag{2}$$

$$\rho \frac{\partial \mathbf{u}}{\partial t} + \rho \mathbf{u} \cdot \nabla \mathbf{u} = \nabla \cdot \boldsymbol{\sigma} + \rho \mathbf{g}. \tag{3}$$

The constitutive equation for the Cauchy stress tensor $\boldsymbol{\sigma}$ is given by

$$\boldsymbol{\sigma} = -p\mathbf{I} + \tau, \tag{4}$$

$$p = p_0 - \mu \operatorname{tr}(\mathbf{D}) = p_0, \tag{5}$$

$$\tau = 2\eta \mathbf{D}^d, \tag{6}$$

in which generalised Newtonian behaviour is assumed for the viscosity:

$$\eta = \eta(p, \mathbf{D}^d). \tag{7}$$

Each variable in Equations (2)–(7) can be written as a product of a dimensionless variable and its characteristic value (see Table I). The ratio ε determines the type of mould geometry; in this paper we limit ourselves to cube-like ($\varepsilon \approx 1$) and oblong ($\varepsilon < 1$) geometries. (The reader may note that since y is rather unconventionally scaled with H instead of L, thin-walled geometries are characterised by $\varepsilon > 1$.) At this point, we will not specify the characteristic value p_{ref} for the pressure yet.

The conservation equations can now be expressed in their dimensionless forms. When normalising all terms in the equation of conservation of momentum with respect to the stationary inertia forces, this yields

Table I. Process variables expressed as products of dimensionless variables (marked with *) and characteristic values

$x = x^*L$	$y = y^*H = y^*\varepsilon L$	$z = z^*H = z^*\varepsilon L$
$u = u^*U$	$v = v^*V = v^*\varepsilon U$	$w = w^*V = w^*\varepsilon U$
$\varepsilon = H/L$		
$t = t^*\tau$	$p = p^*p_{\text{ref}}$	$\mathbf{D}^d = \mathbf{D}^{d*}U/H$
$\rho = \rho^*\rho_0$	$\eta = \eta^*\eta_0$	$\mathbf{g} = \mathrm{g}^*g_0$

The rate-of-deformation tensor $\mathbf{D}^d$ has been scaled with the largest components of $\mathbf{Vu}$ for $\varepsilon \leq 1$, which are $\partial u/\partial y$ and $\partial u/\partial z$.

$$\mathbf{V}\cdot\mathbf{u} = 0, \tag{8}$$

$$Sr\rho\frac{\partial \mathbf{u}}{\partial t} + \rho\mathbf{u}\cdot\mathbf{V}\mathbf{u} = -\frac{p_{\text{ref}}}{\rho_0 U^2}\cdot\mathbf{V}p + \frac{1}{Re}\mathbf{V}(2\eta\mathbf{D}^d) + \frac{1}{Fr}\rho\mathbf{g}, \tag{9}$$

from which the asterisk (*) indicating dimensionless variables has been removed. The dimensionless Reynolds, Strouhal, and Froude numbers are given by

$$Re = \frac{\rho_0 UH}{\eta_0}, \qquad Sr = \frac{L}{\tau U}, \qquad Fr = \frac{U^2}{g_0 L}. \tag{10}$$

The boundary conditions for the Navier–Stokes equations will be discussed separately in Section 2.2.

Characteristic values for injection moulding of polymers are given in Table II. The characteristic time τ is related to the time scale upon which velocity fluctuations of order U occur. In injection moulding, such a fluctuation will only occur immediately after starting the process. As we are not interested in start-up phenomena, τ is very large with respect to L/H and consequently the Strouhal number Sr is very small. The other dimensionless numbers can be determined as

$$Re = \begin{cases} 10^{-3} & \text{for polymer} \\ 10^{2} & \text{for air} \end{cases}, \qquad Fr = 10^{-2}, \tag{11}$$

2.1.1. Polymer domain. For the polymer domain, the Reynolds number indicates that the stationary inertia terms can be neglected. The conservation of momentum equation is now re-scaled with respect to the viscous stress term:

Table II. Characteristic values of the process variables for polymer injection moulding

Variable	Unit	Characteristic value	
		Polymer	Air
ρ_0	kg m^{-3}	10^3	1
η_0	Pa s	10^3	10^{-5}
L	m	10^{-1}	
H	m	10^{-2}	
U	m s^{-1}	10^{-1}	
g_0	m s^{-2}	10	
γ	N m^{-1}	10^{-2}	

$$\frac{p_{\text{ref}}H}{\eta_0 U}\nabla p = \nabla(2\eta \mathbf{D}^d) + \frac{Re}{Fr}\rho \mathbf{g}. \tag{12}$$

The pressure in the polymer is determined by the viscous stresses, therefore, we can define $p_{\text{ref}} = \eta_0 U/H$, yielding a stationary Stokes equation:

$$\nabla p = \nabla(2\eta \mathbf{D}^d) + \frac{Re}{Fr}\rho \mathbf{g}. \tag{13}$$

Whether or not the gravity forces have to be taken into account, is determined by

$$\frac{Re}{Fr} = \frac{\rho g_0 HL}{\eta_0 U} = \frac{10^3 10^1 H 10^{-1}}{10^3 10^{-1}} = 10H. \tag{14}$$

Hence if $\mathcal{O}(H) = \mathcal{O}(L) = 10^{-1}$ m, then the gravity forces have to be taken into account; otherwise, if H is considerably smaller than 10^{-1} m, then the gravity forces can be neglected. Conforming to injection moulding practice, we choose H to be of order 10^{-2} m, thus further limiting ourselves to oblong geometries, but the inclusion of gravity forces does not impose significant difficulties.

2.1.2. Air domain. For the air domain, the viscous forces can be neglected and the scaling of Equation (9) can be maintained. In this case, the characteristic pressure can be defined as $p_{\text{ref}} = \rho_0 U^2$, yielding

$$\rho \mathbf{u}\cdot\nabla\mathbf{u} = -\nabla p + \frac{1}{Fr}\rho \mathbf{g}. \tag{15}$$

This implies that we would have to solve a non-linear (Euler) equation, which, however, would yield a pressure drop in the air domain that is considerably smaller than in the polymer domain (which can be seen from a comparison of the pressure scaling for both materials). By replacing the air with a fictitious fluid, of which the viscosity is of order 10^{-3} of the polymer viscosity and which has the same mass density as air, the Reynolds number for the fictitious fluid domain would reduce to $Re = 10^{-3}$. Hence the inertia terms in the fictitious fluid domain can be neglected, while the pressure drop is still negligibly small compared with the pressure drop in the polymer domain. As a result, we can apply the stationary Stokes equation (Equation 13) for the entire computational domain.

Consequently, in the sequel of this paper the words 'polymer' and 'air' will denote Newtonian fluids with viscosities of order 10^3 and 1 Pa s, and densities of order 10^3 and 1 kg m^{-3} respectively.

2.2. Boundary conditions

We define a domain Ω covering the mould, with boundaries Γ_e, Γ_w and Γ_v designating the mould entrance, the mould walls, and the air vents. At the mould entrance, either the injection flow rate or the normal stress (i.e. the injection pressure) is prescribed. Wherever the mould wall is covered with polymer, a no-slip condition is imposed. The physically correct boundary conditions near the moving contact line, however, cannot be uniquely determined, since the physics of this phenomenon are still not completely understood, [13,14] and will probably demand modelling at scales much smaller than any mesh size that is manageable for mould filling simulations [15]. As a no-slip boundary condition in the air would prevent the polymer from contacting the mould wall, we have chosen to prescribe a free-slip condition downstream of the flow front, thus enabling the contact point to move freely. Hence, the boundary condition along the mould walls is a function of the type of material. This has been

implemented by using an adjustable Robin boundary condition for the (dimensionless) velocity and stress components $\mathbf{u}_t$ and $\boldsymbol{\sigma}_t$ in tangential direction:

$$a\mathbf{u}_t + \boldsymbol{\sigma}_t = 0 \quad \forall \mathbf{x} \in \Gamma_w \cup \Gamma_v, \tag{16}$$

in which the dimensionless 'Robin penalty parameter' a is defined as

$$a = a(c) = \begin{cases} \text{large } (\geq 10^4) & \text{if } c \geq 0.5 \text{ no} - \text{slip} \\ 0 & \text{if } c < 0.5 \text{ free} - \text{slip} \end{cases}. \tag{17}$$

(From Equation (16) it can be derived that a scales with η_0/H.)

The mould walls are impermeable, except at the air vents Γ_v where the air is allowed to leave the mould, yielding the following boundary conditions for the velocity and stress component u_n and σ_n in normal direction:

$$u_n = 0 \quad \forall \mathbf{x} \in \Gamma_w, \tag{18a}$$

$$au_n + \sigma_n = 0 \quad \forall \mathbf{x} \in \Gamma_v, \tag{18b}$$

in which a is again given by Equation (17).

2.3. Interfacial conditions

From a physical point of view, two more boundary conditions hold for the flow front, namely immiscibility and conservation of momentum. The immiscibility condition is already implied by the 'conservation of identity' (Equation 23). The conservation of momentum at the interface is expressed as [16]

$$(\boldsymbol{\sigma}_2 - \boldsymbol{\sigma}_1) \cdot \mathbf{n}_{12} = \gamma_{12} \kappa \mathbf{n}_{12}, \tag{19}$$

in which the subscripts 1 and 2 denote the polymer and the fictitious fluid, and γ_{12}, κ, and $\mathbf{n}_{12}$ denote the interfacial tension, the interface curvature, and the normal vector to the interface respectively. Using Equation (6) and introducing dimensionless variables, Equation (19) can be written as

$$(\boldsymbol{\sigma}_2^* - \boldsymbol{\sigma}_1^*) \cdot \mathbf{n}_{12}^* = \frac{1}{Ca} \gamma_{12}^* \kappa \mathbf{n}_{12}^*, \tag{20}$$

in which Ca is the Capillary number, i.e. the ratio of viscous and interfacial forces, defined as

$$Ca = \frac{\eta_0 U}{\gamma}, \tag{21}$$

in which η_0 is the characteristic viscosity of the highly viscous fluid, U is the characteristic velocity, and γ is the interfacial tension. For injection moulding of polymers, the Capillary number is of the order 10^4, indicating that interfacial forces can be neglected. Thus Equation (19) reduces to (when omitting the asterisk from the dimensionless variables)

$$(\boldsymbol{\sigma}_2 - \boldsymbol{\sigma}_1) \cdot \mathbf{n} = 0, \tag{22}$$

which is already taken care of by the overall conservation of momentum equation (9), since the material properties are continuous functions of c at the interface. As a result, the phenomena at the flow front have already been taken into account in our model.

Although we are able to employ generalised Newtonian viscosity behaviour in our simulations, we will limit ourselves to Newtonian behaviour in this paper, since the fountain flow effect is determined by the continuity equation, more than by the constitutive behaviour [17].

2.4. Material label convection

The material labels that are used to distinguish polymer from air are convected through the mould with velocity **u**. Hence a pure (passive scalar) convection equation describes the evolution of the material label distribution; in its dimensionless form, it reads

$$\dot{c} = 0 \Leftrightarrow Sr \frac{\partial c}{\partial t} + \mathbf{u} \cdot \nabla c = 0. \tag{23}$$

In fact, this can be regarded as a conservation equation of particle identity. Initially, c is set to zero in the entire domain Ω, and only a boundary condition at the flow entrance is needed:

$$c = 1 \quad \forall \mathbf{x} \in \Gamma_e, \qquad t > 0, \tag{24}$$

The boundary condition for the convection equation can also be the time of entrance (injection time) or one of the entrance co-ordinates. Equation (23) can then be used to perform particle tracking [18]. Some examples will be shown in Section 4.

The material properties as they appear in the Stokes equation can now be determined locally as a function of the material label. The mould filling problem can thus be simulated by solving Equations (13) and (23) and updating the material properties at every time step.

3. NUMERICAL METHODS

The model has been implemented in the finite element package SEPRAN [19]. This section gives a short description of the implementation.

3.1. The Stokes equation

A standard Galerkin finite element method is used to solve the continuity equation (8) and the Stokes equation (13), which can be written after spatial discretisation as

$$L \underset{\sim}{u} = 0, \tag{25}$$

$$S \underset{\sim}{u} + L^T \underset{\sim}{p} = \underset{\sim}{f}, \tag{26}$$

in which $\underset{\sim}{f}$ is the right-hand-side vector containing the essential boundary conditions and any volume forces, and

$$S_{ij} = \frac{1}{Re} \int_\Omega \eta \nabla \phi_i \cdot \nabla \phi_j \, d\Omega, \qquad L_{ij} = -\int_\Omega \psi_i \nabla \phi_j \, d\Omega,$$

and ϕ_i and ψ_i are the shape functions for the velocity and the pressure, respectively.

For 2D problems, a penalty function method in combination with a direct solver is used to solve this system of equations. In the case of 3D problems, the combination of an integrated method and an iterative (conjugate gradient squared (CGS)) method is applied in order to avoid excessive CPU time and memory usage [20].

The elements used are so-called Cronzeix–Raviart ($Q_2^+ - Q_1$) rectangular elements, that employ an extended quadratic approximation for the velocity and a linear approximation, which is discontinuous at the element boundaries, for the pressure [21].

The material parameters are initially defined as discontinuous functions of the material labels, e.g. for viscosity

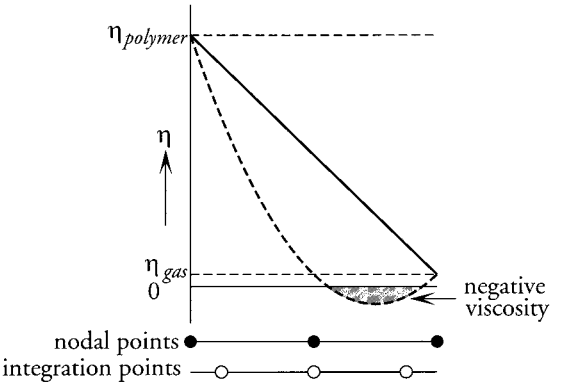

Figure 1. Piece-wise linear interpolation of viscosity on a quadratic element to avoid negative values: - - - = original function, — = interpolated function.

$$\eta = \eta(c) = \begin{cases} \eta_{\text{polymer}} & \text{if } c \geq 0.5 \\ n_{\text{fictitious}} & \text{if } c < 0.5 \end{cases} \tag{27}$$

The use of quadratic shape functions may then lead to negative values of the material property at the elements' integration points (see Figure 1). This is avoided by piece-wise linear interpolation of the material parameter at the midpoints of elements containing the flow front [11].

3.2. The convection equation

The convection equation for the material labels is solved with the finite element method using an streamline–upwind Petrov–Galerkin (SUPG) scheme incorporating Shakib's parameter suggested for time-dependent problems [22,23].

Applying spatial discretisation, the convection equation can be written in the form

$$\mathrm{M}\,\dot{\underset{\sim}{c}} + \mathrm{N}(\mathbf{u})\,\underset{\sim}{c} = 0, \tag{28}$$

in which M is the mass matrix and N(**u**) is the convection matrix. Temporal discretisation with a finite difference θ-method yields

$$\mathrm{M}\,\frac{\underset{\sim}{c}^{n+1} - \underset{\sim}{c}^{n}}{\Delta t} + \theta\,\mathrm{N}(\mathbf{u}^{n+1})\,\underset{\sim}{c}^{n+1} + (1-\theta)\mathrm{N}(\mathbf{u}^{n})\,\underset{\sim}{c}^{n} = 0, \tag{29}$$

in which the superscripts $n+1$ and n indicate consecutive time steps. This can be approximated by a two-step procedure, yielding a set of equations that can be solved more efficiently:

$$\left(\frac{\mathrm{M}}{\theta\,\Delta t} + \mathrm{N}(\mathbf{u}^{n+\theta})\right)\underset{\sim}{c}^{n+\theta} = \frac{\mathrm{M}}{\theta\,\Delta t}\,\underset{\sim}{c}^{n}, \tag{30}$$

$$\underset{\sim}{c}^{n+1} = \frac{1}{\theta}\,(\underset{\sim}{c}^{n+\theta} - (1-\theta)\,\underset{\sim}{c}^{n}). \tag{31}$$

For the time discretisation, a modified version of the Crank–Nicolson scheme ($\theta = 0.5$) is used: θ is set to $0.5 + \alpha\overline{\Delta t}$, in which $\overline{\Delta t}$ is the dimensionless time step defined as $\overline{\Delta t} = \Delta t/(t_{\text{end}} - t_0)$ and α is a small positive real number (e.g. $\alpha = 0.03$). This suppresses oscillations in c without affecting the order of accuracy.

After every time step, the material labels are rounded off to either unity or zero everywhere, except in the elements containing an interface, where the original values of the material labels are retained. Hence, possible oscillations in the material label field are suppressed.

4. RESULTS

In order to show that the method described in this paper is suitable for the simulation of moulding processes, four simulation results are presented:

1. Filling of an axisymmetric cylinder with polymer; this is, strictly speaking, a two-dimensional problem.
2. Flow front development in a (two-dimensional) bifurcation.
3. Three-dimensional flow in a rectangular cavity.
4. Expelling a viscous fluid from a tube by a less viscous fluid, as described by Taylor [24].

In all simulations, a parabolic velocity profile at the entrance is prescribed.

4.1. Filling of an axisymmetric cylinder

As an initial test for the model, the injection of polymer into an axisymmetric cylinder was simulated, with the geometry and the parameters given in Figure 2(a) and Table III. A parabolic velocity profile is prescribed at the flow entrance Γ_e, causing the cylinder to be filled in 1.0 s. An air vent has been defined at Γ_v. A mesh of 40×10 quadrilateral, axisymmetric elements (along the cylinder length and radius, respectively) was used.

To visualise the fountain flow effect, time labels were introduced: particles entering the mould are given their injection times as labels (see Section 2.4). These are convected through the mould analogously to the material labels. The air that is initially present in the mould is given a negative time label.

The time label distribution after 70% filling (Figure 2(c)) clearly shows the fountain flow effect: polymer material has approached the flow front from the centre and has been diverted towards the wall. This results in the typical 'V'-shaped material label field near the mould wall that have also been encountered in experiments [17,25]. It can also be seen from the pressure contours in Figure 2(d), that the air does not contribute significantly to the pressure drop. The polymer mass loss in this simulation was $< 2\%$.

Table III. Process parameters for the simulations

Mould type	Axisymmetric cylinder	Bifurcation	3D box
Dimensions	$L = 100$ mm $R = 5.0$ mm	see Figure 3	$L = 100$ mm $W/2 = 15$ mm $H/2 = 5$ mm
Viscosity ratio	10^3	10^3	10^3
Filling time	1.0 s	1.0 s	1.0 s
# Elements	400	1710	980
# Time steps	100	200	100

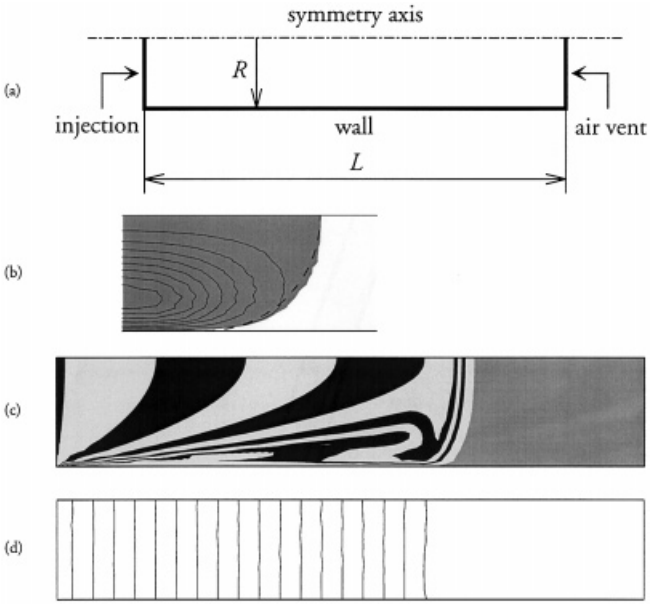

Figure 2. Simulation of filling of an axisymmetric tube (results shown for 70% filling). (a) Computational domain. (b) Detail of the flow front area: material labels (grey = polymer, white = air), and streamlines relative to the flow front velocity. The dashed line corresponds to a semi-spherical flow front. (c) Time label distribution visualising the fountain flow effect (black and light grey = polymer, dark grey = air). (d) Pressure contour lines at equal pressure intervals. (Note that scaling of the width-to-length ratio has distorted the semi-spherical shape of the flow front in Figure 3(c).)

A detail of the flow front and the streamlines *relative to the moving flow front* are depicted in Figure 2(b). The phrase 'fountain flow' becomes immediately clear from these streamlines. For Newtonian fluids in an axisymmetric tube, the flow front was found to be semi-spherical [26]. Comparison with the (quarter) circle drawn in Figure 2(b) shows that the computed interface is indeed not far from semi-spherical.

From the results for filling of an axisymmetric tube, we conclude that the method presented in this paper is capable of tracking the material interface in mould filling processes governed by viscous effects. Moreover, the model is also able to deal with the fountain flow effect.

4.2. Flow in a bifurcation

Flow bifurcations are common in mould filling processes, especially in polymer injection moulding. Therefore, we have tested whether the method presented in this paper is able to deal with the bifurcation that is present in the T-shaped two-dimensional mould shown in Figure 3(a), which is taken from Zoetelief *et al*. [18]. Of the two downstream branches, the top branch has a lower flow resistance than the right branch, since it is both wider and shorter. An extra air vent at the bifurcation is necessary to prevent air entrapment. The process and material parameters are similar to the previous case (see Table III).

Figure 3(b–d) show the time label fields at three different filling stages. In Figure 3(b) the flow front has just started to split between the two downstream branches. Due to the lower flow resistance, the flow front in the top branch runs ahead (Figure 3(c)). After the top branch has been filled, all material will flow into the right (narrow) branch (Figure 3(d)). It can even be seen that material in the entrance of the top branch is eventually dragged into the right branch. Due to a mass loss of 2.8%, the mould is not entirely filled at $t = 1.0$ s.

4.3. Flow in a three-dimensional rectangular cavity

Since the modelling described in Sections 2 and 3 did not contain any restriction to two-dimensional flows only, the method should be directly applicable to three-dimensional mould filling simulations. Figure 4(a) shows a three-dimensional rectangular cavity, of which only one-quarter is meshed because of two-fold symmetry (Figure 4(b)). Due to the increase in computing time and memory usage, this mesh is somewhat coarser than in the two-dimensional situations presented above. To (partly) compensate for this coarseness, the mesh is refined towards mould walls, where both the velocity gradients and the injection time label gradients are large. With process and material parameters being similar to the previous cases (see Table III), the simulation for a $20 \times 7 \times 7$ mesh took nearly 6 h of CPU-time on a SGI Power Challenge R10000.

Figure 4(c,d) show the three-dimensional fountain flow effect in both planes of symmetry. The relatively coarse mesh in the x- and z-directions together with the large time label gradients near the mould walls gives rise to oscillations in the injection time label field, as can be seen in cross-section plots made at $y = 0.3L$ and $y = 0.7L$ (Figure 4(e,f)). Such oscillations do not occur in the material label distribution, because all material label gradients are continuously updated by setting them to either zero or one outside the interface regions. The mass loss of polymer is 3.5%, which is nearly twice as much as in the axisymmetric cylinder case.

These three-dimensional simulation results show that the pseudo-concentration method, as it is employed in this paper, is indeed suitable for three-dimensional flow simulations.

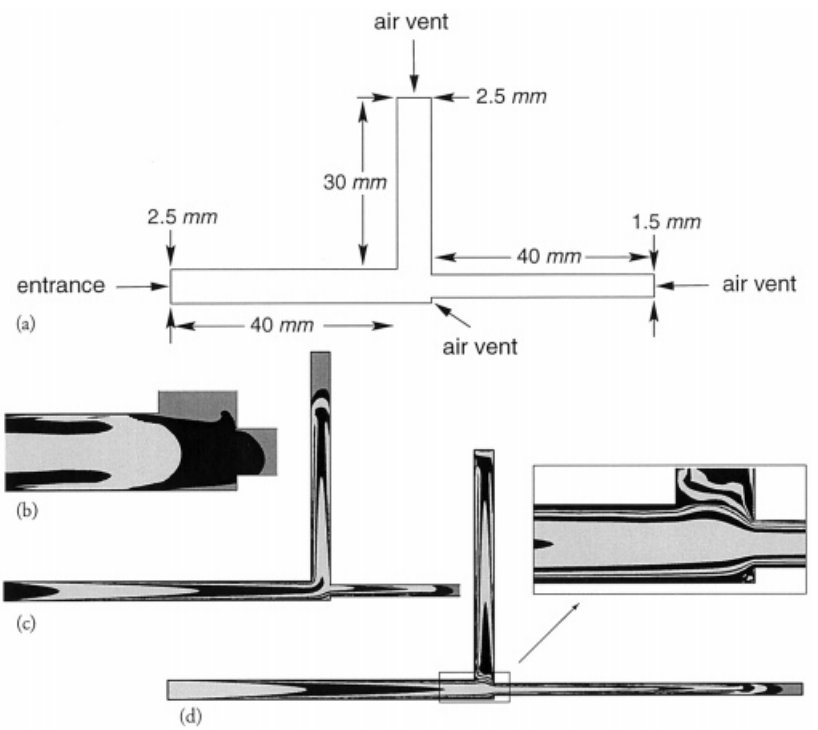

Figure 3. Simulation of flow in a two-dimensional bifurcation. (a) Geometry. (b) Detail of injection time label distribution at 0.45 s. (c) Injection time label distribution at 0.8 s. (d) Injection time label distribution at 1.0 s. (Black and light grey = polymer, dark grey = air.)

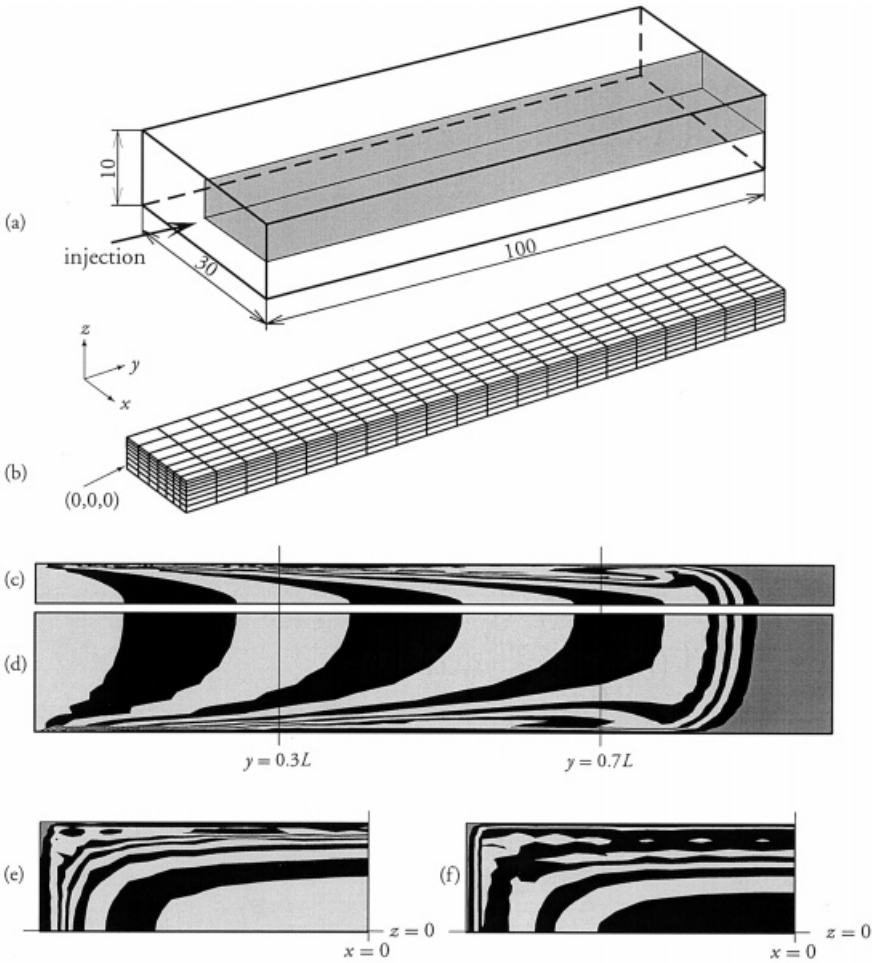

Figure 4. Filling simulation for a three-dimensional rectangular cavity (results shown for 90% filling). (a) Geometry. (b) Computational mesh (corresponding to grey quarter of the geometry shown above). (c,d) Injection time labels at planes of symmetry (c) $x = 0$ and (d) $y = 0$. (e,f) Injection time labels at the cross-sectional planes (e) $y = 0.3L$ and (f) $y = 0.7L$.

4.4. Expelling a viscous fluid from a tube

The question of displacement of a viscous fluid in a tube by a less viscous fluid was aroused by Fairbrother and Stubbs [27] in 1935 and has received considerable attention since [24,28–32]. In fact, it is the reverse problem of mould filling: the 'mould' is initially filled with a viscous fluid, and a less viscous fluid is injected. Fairbrother and Stubbs found that the injected fluid did not expel the original fluid entirely, as a considerable fraction was left behind at the tube wall. This fraction, given by

$$m = \frac{A_{\text{original fluid}}}{A_{\text{tube}}}, \tag{32}$$

in which A is the cross-sectional area perpendicular to the centre line of the tube, was found to be a function of the Capillary number only (i.e. for Newtonian fluids). Taylor [24] suggested that m reaches and an asymptotic value of *at least* 0.56 for large Capillary numbers (i.e.

negligible surface tension). Cox [28] experimentally found m to be 0.60 for tetrachloromethane penetrating into golden syrup (a sucrose solution) for $Ca > 10$. Halpern and Gavern [31] used a boundary element method for their numerical analysis of the problem; for an inviscid gas at constant pressure penetrating into an incompressible Newtonian fluid, they neglected inertia forces and found $m = 0.58$ for $Ca = 10^4$, which is similar to the experimental result of Poslinski *et al.* [32].

We have simulated the displacement of a viscous fluid by a gas by injecting air into a tube filled with polymer. As such, this simulation is similar to the filling of a tube described in Section 4.1, but with 'polymer' and 'air' reversed. Furthermore, the polymer was allowed to leave the mould at the mould exit assigned by Γ_v (Figure 2(a)).

This case also serves as a convergence test for the pseudo-concentration method presented in this paper. The convergence of the residual fluid fraction m has been taken as the convergence criterion, as it is directly related to the computed position of the air–polymer interface. Assuming that a mesh of 128×32 elements (over L and R, respectively) and a time step of 3.125×10^{-4} s yields a converged solution (which can be easily checked afterwards), we have carried out two sequences of simulations: one with an increasing time step, and another one with a decreasing number of elements (keeping, the mesh and the time step constant respectively). Having thus found that a mesh of 32×8 elements yields a sufficiently converged result (see Table IV), the time step has again been increased. A time step size of 1.25×10^{-2} for this mesh appears to be sufficient. Even a mesh of 16×8 elements seems to yield a sufficiently converged solution, but gives rise to significant oscillations in the velocity field.

Figure 5(a) shows that an air core has penetrated into the polymer, leaving a polymer fraction of $m = 0.59$ behind, which is in agreement with the values found in the literature. The streamlines in Figure 5(b) match well with the streamlines predicted by Taylor [24] and visualised by Cox [29].

5. CONCLUSIONS

In this paper, we have adopted the pseudo-concentration method to develop a simulation program for three-dimensional mould filling. To simulate the advancement of the flow front, the boundary condition at the mould wall had to be split into two parts: a no-slip boundary

Table IV. Residual fluid fraction m as a function of element size and time step for the case of a viscous (Newtonian) fluid being expelled from a cylinder by a less viscous fluid

# Elements	Time step [s]				
	3.125×10^{-4}	6.25×10^{-4}	1.25×10^{-3}	2.5×10^{-3}	5×10^{-3}
128×32	0.601	0.597	0.583	0.550	
64×32	0.599				
64×16	0.601				
32×16	0.598				
32×8	0.596	0.593	0.593	0.581	0.555
16×8	0.597*	0.597*	0.596*		
16×4	0.612*				

Results marked with an asterix exhibit oscillations in the velocity field.

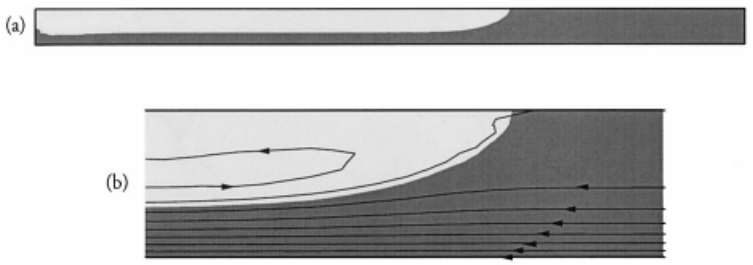

Figure 5. Simulation of driving a viscous fluid out of an axisymmetric tube (the fluid is allowed to leave the mould at the right end). (a) Material label distribution after $t = 0.3$ s (grey = polymer, white = air). (b) Detail of the flow front area, with streamlines relative to the flow front velocity.

condition was imposed for the filling fluid region, whereas a free-slip boundary condition was prescribed for the fictitious fluid region. This was implemented as a material (i.e. pseudo-concentration) dependent Robin boundary condition. For both fluids, the mould wall was impermeable, except at specified air vents, where the fictitious fluid was allowed to escape.

The model presented in this paper has proven to work well for the filling of both two- and three-dimensional moulds: both the advancement of the flow front, including the moving contact points/lines, and the fountain flow effect, which is characteristic for viscous flow, emerge very clearly from the simulations. Moreover, the model is also able to simulate the penetration of gas into a viscous fluid, which can be considered the reverse problem of mould filling, yielding a residual fluid fraction of 0.59.

From these results, we consider the pseudo-concentration method as a promising technique for mould filling simulations, provided the boundary conditions near the moving flow front are chosen properly. Three-dimensional simulations do need a considerable amount of CPU time (6 h for a simple geometry), but in our opinion, this is still to be preferred over three-dimensional remeshing.

ACKNOWLEDGMENTS

This work is financially supported by the Graduate School Polymer Technology Netherlands (PTN).

REFERENCES

1. C. Huh and L.E. Scriven, 'Hydrodynamic model of steady movement of a solid/liquid/fluid contact line', *J. Colloid Interface Sci.*, **35**, 85–101 (1971).
2. J.M. Floryan and H. Rasmussen, 'Numerical methods for viscous flows with moving boundaries', *Appl. Mech. Rev.*, **42**, 323–340 (1989).
3. R.W. Lewis, A.S. Usmani and J.T. Cross, 'Efficient mould filling simulation in castings by an explicit finite element method', *Int. J. Numer. Methods Fluids*, **20**, 493–506 (1995).
4. M. Medale and M. Jaeger, 'Numerical simulation of incompressible flows with moving interfaces', *Int. J. Numer. Methods Fluids*, **24**, 615–638 (1997).
5. E. Thompson, 'Use of pseudo-concentrations to follow creeping viscous flows during transient analysis', *Int. J. Numer. Methods Fluids*, **6**, 749–761 (1986).
6. C.W. Hirt and B.D. Nichols, 'Volume of Fluid (VOF) method for the dynamics of free boundaries', *J. Comput. Phys.*, **39**, 201–225 (1981).
7. W. Rose, 'Fluid–fluid interfaces in steady motion', *Nature*, **191**, 242–243 (1961).
8. S. Bhattacharji and P. Savic, 'Real and apparent non-Newtonian behavior in viscous pipe flow of suspensions driven by a fluid piston', *Proc. 1965 Heat Transfer and Fluid Mechanics Institute*, 1965, pp. 248–262.
9. J.M. Castro and C.W. Macosko, 'Studies of mold filling and curing in the reaction injection moulding process', *AIChE J.*, **28**, 250–260 (1982).

10. A.S. Usmani, J.T. Cross and R.W. Lewis, 'A finite element method for the simulations of mould filling in metal casting and the associated heat transfer', *Int. J. Numer. Methods Eng.*, **35**, 787–806 (1992).
11. A. Fortin, A. Béliveau and Y. Demay, 'Numerical solution of transport equations with applications to non-Newtonian fluids', in M.M. Marquez and J. Rodriguez (Eds.), *Trends in Applications of Mathematics to Mechanics* Longman, Harlow, 1995.
12. J.-F. Hétu, Y. Lauzé and A. Garcia-Rejon, 'Three-dimensional finite element simulation of mold filling processes', in S.-F. Shen and P. Dawson (Eds.), *Simulation of Materials Processing: Theory, Methods and Applications* (*Numiform 95*), Balkema, Rotterdam, 1995, pp. 1135–1140.
13. E.B. Dussan V, 'On the spreading of liquids on solid surfaces: static and dynamic contact lines', *Annu. Rev. Fluid Mech.*, **11**, 371–400 (1979).
14. P.G. de Gennes, 'Wetting: statics and dynamics', *Rev. Mod. Phys.*, **57**, 827–863 (1985).
15. A.J.J. van der Zanden, 'The hydrodynamics of a moving fluid–liquid contact line', *Ph.D. Thesis*, Eindhoven University of Technology, 1993.
16. G.K. Batchelor, *An Introduction to Fluid Mechanics*, Cambridge University Press, Cambridge, 1967.
17. D.J. Coyle, J.W. Blake and C.W. Macosko, 'The kinematics of fountain flow in mold-filling', *AIChE J.*, **33**, 1168–1177 (1987).
18. W.F. Zoetelief, G.W.M. Peters and H.E.H. Meijer, 'Numerical simulation of the multi-component injection moulding process', *Int. Polym. Process.*, **XII**, 216–227 (1997).
19. A. Segal, *SEPRAN manual*, Ingenieursbureau SEPRA, Leidschendam, 1996.
20. A. Segal and C. Vuik, 'A simple iterative linear solver for the 3D incompressible Navier–Stokes equations discretized by the finite element method', *Technical Report 95-64*, Delft University of Technology, 1995.
21. C. Cuvelier, A. Segal and A.A. van Steenhoven, *Finite Element Methods and Navier–Stokes Equations*, Reidel, Dordrecht, 1986.
22. A.N. Brooks and T.J.R. Hughes, 'Streamline upwind/Petrov–Galerkin formulations for convection dominated flows with particular emphasis on the incompressible Navier–Stokes equations', *Comput. Methods Appl. Mech. Eng.*, **32**, 199–259 (1982).
23. F. Shakib, 'Finite element analysis of the compressible Euler and Navier–Stokes equations', *Ph.D. Thesis*, Stanford University, Stanford, CA, 1989.
24. G.I. Taylor, 'Deposition of a viscous fluid on the wall of a tube', *J. Fluid Mech.*, **10**, 161–165 (1961).
25. L.R. Schmidt, 'A special mold and tracer technique for studying shear and extensional flows in a mold cavity during injection molding', *Polym. Eng. Sci.*, **14**, 797–800 (1974).
26. R.L. Hoffman, 'A study of the advancing interface. I. Interface shape in liquid–gas systems', *J. Colloid Interface Sci.*, **50**, 228–241 (1975).
27. F. Fairbrother and A.E. Stubbs, 'Studies in electro-endosmosis. Part VI. The "bubble-tube" method of measurement', *J. Chem. Soc.*, **1**, 527–529 (1935).
28. B.G. Cox, 'On driving a viscous fluid out of a tube', *J. Fluid Mech.*, **14**, 81–96 (1962).
29. B.G. Cox, 'An experimental investigation of the streamlines in viscous fluid expelled from a tube', *J. Fluid Mech.*, **20**, 193–200 (1964).
30. D.A. Reinelt and P.G. Saffman, 'The penetration of a finger into a viscous fluid in a channel and tube', *SIAM J. Sci. Stat. Comput.*, **6**, 542–561 (1985).
31. D. Halpern and D.P. Gaver III, 'Boundary element analysis of the time-dependent motion of a semi-infinite bubble in a channel', *J. Comput. Phys.*, **115**, 366–375 (1994).
32. A.J. Poslinski, P.R. Oehler and V.K. Stokes, 'Isothermal gas-assisted displacement of viscoplastic liquids in tubes', *Polym. Eng. Sci.*, **35**, 877–892 (1995).

